



VICTORIA UNIVERSITY
MELBOURNE AUSTRALIA

Experimental behaviour of high-strength concrete deep beams with web openings

This is the Accepted version of the following publication

Doh, Jeung-Hwan, Yoo, Tae-Min, Guan, Hong and Fragomeni, Sam (2011)
Experimental behaviour of high-strength concrete deep beams with web openings. *The structural design of tall and special buildings*. ISSN 1541-7808

The publisher's official version can be found at
<http://onlinelibrary.wiley.com/doi/10.1002/tal.718/pdf>
Note that access to this version may require subscription.

Downloaded from VU Research Repository <https://vuir.vu.edu.au/8911/>

EXPERIMENTAL BEHAVIOUR OF HIGH STRENGTH CONCRETE DEEP BEAMS WITH WEB OPENINGS

TAE-MIN YOO¹, JEUNG-HWAN DOH^{1*}, HONG GUAN¹ AND SAM FRAGOMENT²

¹*Griffith School of Engineering, Griffith University Gold Coast Campus, Queensland 4222, Australia*

²*School of Engineering and Science, Victoria University, Melbourne, Australia*

SUMMARY

This paper focuses on an experimental study undertaken on High Strength Concrete (HSC) deep beams with various opening sizes and locations on the web. The test covers a wide scope of variables that have not been investigated in previous research. Apart from highlighting the experimental setup, failure loads and typical crack patterns of the test specimens are also reported. Experimental results are then compared with predictions using currently available design methods. The comparison indicates that the predictions using current design methods can overly underestimate or sometimes overestimate the ultimate strength of these HSC deep beams. Further, the reduction of ultimate strengths due to the existence of web openings is not considered adequately in these design methods. To rectify the shortcomings of current design formulae, a new design equation is proposed and compared with the experimental results and those from previous studies on the related topics. The accuracy and reliability of the proposed new equation is subsequently confirmed. Based on the outcome of this work, more experimental tests with various opening configurations including shape and location of web openings are recommended for future study.

1. INTRODUCTION

The utilisation of deep beams within structural engineering practice has grown substantially over the last four decades. More specifically, there has been an increased practise of including deep beams in the design of high-rise buildings, offshore structures, and foundations. A deep beam loaded at any point or loaded continuously over its span distributes this load to its supports, and this can aid in the provision of more open space in a structure when compared with other design methods. Although reinforced concrete deep beams are of considerable interest in structural engineering practice, major codes of practice such as AS3600-2009, ACI318-08 and CSA 1984, still offer little guidance on the design of high strength concrete deep beams, particularly when openings in the web region are provided for essential services and accessibility (Kong, 1990). The need for an accurate design method for deep beams with openings is therefore becoming increasingly necessary.

Web openings are introduced to accommodate services including air-conditioning ducts and cables to save space, as these would otherwise be located below the deep beam. An opening produces geometric discontinuity within the beam and affects the nonlinear stress

* Correspondence to: Jeung-Hwan Doh, Griffith School of Engineering, Griffith University, Gold Coast campus, QLD, Australia, 4222. E-mail: J.doh@griffith.edu.au

distribution over the depth of the beam. The inclusion of web openings decreases the ultimate strength of a deep beam that can be attributed to the reduction of concrete mass acting in compression and the opening acting as a stress raiser for shear crack propagation. This is particularly evident when the opening is located along the critical load path of a deep beam.

Current code of standards such as AS3600-2009 and ACI318-2009 devote separate chapters to deep beam design, recommended the use of strut-and-tie methods. However, current codes of standards are only intended for solid deep beams.

Web openings in a deep beam significantly affect its structural behaviour as demonstrated in previous studies (Kong and Sharp 1977; Kong *et al.* 1978; Mansur and Alwis 1984; Ray 1990; Almeida and Pinto 1999; Ashour and Rishi 2000; Maxwell and Breen 2000; Tan *et al.* 2003; Yang *et al.* 2006; Yang and Ashour 2008). A simple structural idealization for predicting the ultimate shear strength of deep beams with web openings was proposed some thirty years ago based on a series of laboratory testing conducted by Kong and Sharp (1977) and Kong *et al.* (1978) and extended upon by Tan *et al.* (2003). The structural idealization shows the lower and upper paths of load transfer when a web opening is present. It offers a good indication of the ultimate load-carrying capacity of the beam which is affected by the size and location at which the natural load path is interrupted by an opening (Guan and Doh, 2007).

Even if many researchers have conducted extensive experimental tests on the simply supported deep beams with various web opening configurations, there are still gaps to rectify the limitations on the previous study. Table 1 presents summary of previously available tests on the simply supported deep beams with web openings.

Yang *et al.* (2006) tested 32 high strength concrete deep beams with and without web openings under two-point loading. The variables included concrete strength, width and depth of opening and shear span-to-depth ratio. The authors found that Kong and Sharp's (1977) equation for deep beams with web openings became more conservative with the increase in concrete strength, and Tan *et al.*'s (2003) equation was less conservative. It is also interesting to note that as the shear span-to-depth ratio increased from 0.5 to 1.0 in normal strength and high strength concrete beams, both equations overestimated the shear strength of the deep beams with web openings. This is a concern where deep beams with web openings need to be utilised that comprise of higher shear-span to depth ratios, thus presenting a limitation to these equations.

In recent attention, Ashour and Yang (2008) conducted extensive review on the application of plasticity theory to reinforced concrete deep beams with and without openings. Authors concluded that the strut-and-tie models are generally more difficult to develop for deep beams with web openings than the mechanism approach.

Although these complicated stress states have been reported on in the past, most research has been limited to lightweight and normal strength concrete, the web openings have been very large when compared to the smaller shear-span to depth ratios < 1 .

Hence, the purpose of this study is to investigate the behaviour of high strength concrete deep beams with various web opening sizes and locations. To achieve this, an experimental program has been undertaken to obtain data that includes the ultimate load, crack patterns and failure modes.

This paper details the test procedure and analysis of forty three (43) simply supported high strength concrete deep beams with various web opening sizes and locations. These beams are split into three groups to investigate a variety of geometric parameters relating to different behaviour characteristics of the beams. Data obtained from testing are then compared to predicted results using methods from Kong *et al.* (1978), Kong and Sharp (1977) and Tan *et al.* (2003). Note that the effects of web reinforcements are not considered in this study. Also

2. CURRENT DESIGN FORMULA FOR DEEP BEAM WITH WEB OPENINGS

Based on experimental studies, Kong *et al.* (1970, 1978) and Kong and Sharp (1973, 1977) derived design equations for normal and lightweight concrete deep beams with and without web openings. The ultimate shear strength equations for reinforced concrete deep beams are:

$$Q_{ult} = C_1 \left[1 - 0.35 \frac{x}{D} \right] f_t b D + C_2 \sum A_w \frac{y}{D} \sin^2 \alpha \quad (1)$$

for solid deep beam, and

$$Q_{ult} = C_1 \left[1 - 0.35 \frac{k_1 x}{k_2 D} \right] f_t b k_2 D + \sum \lambda C_2 A_w \frac{y_1}{D} \sin^2 \alpha_1 \quad (2)$$

for deep beam with web opening

The geometric notations are illustrated in Figure 1.

Kong and Sharp (1973, 1977) and Kong *et al.* (1978) made significant contributions to the development of the British Standard and the first term on the right side of Eq. (1) and Eq. (2) expresses the load capacity of a strut. When an opening is in the natural loading path, the first term considers the lower load path. The second term on the right side of the equation articulates the contribution of reinforcement in deep beams. It should be noted however, that these equations are only applicable for concrete strengths less than 46 MPa.

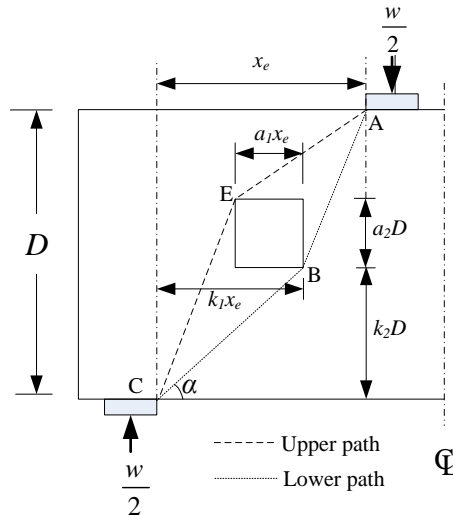


Figure 1. Notation for size and location of opening (half length) (Kong and Sharp, 1977).

Tan *et al.* (1995, 1997 & 2003) and Leong and Tan (2003) investigated the effects of high strength, shear span to depth ratios and web reinforcement ratios of the beams using both an experimental program and numerical analysis. The design shear strength for high strength concrete deep beams is

$$V_n = \frac{1}{\frac{\sin 2\theta_s}{f_t A_c} + \frac{1}{f'_c A_{str} \sin \theta_s}} \quad (3)$$

$$\text{where } f_t = \frac{2A_s f_y \sin \theta_s}{A_c} + \frac{2A_w f_{yw} \sin(\theta_s + \theta_w)}{A_c} \cdot \frac{d_w}{d} + f_{ct} \quad (4a)$$

$$\text{and } \tan \theta_s = \frac{h - \frac{l_a}{2} - \frac{l_b}{2}}{a} \quad (4b)$$

Eq. (2) has limitation on the web opening size and location with respect to the x/D ratio within the 0.25 to 0.4 range. However Eq. (3) does not give any design limitations in regards to the opening size, location or orientation of the opening size; or for that fact, the geometry of the beam itself, including the x/D or L/D ratio. Either they have not considered the effect of these variables, or they are confident that the equation will work under any circumstance.

Although Yang et al. (2006) supports the use of these two equations for high strength concrete deep beams with web openings, the authors noted that Eq. (1) and Eq. (2) were very conservative with the increase in concrete strength, thus the design of these concrete beams is less economical. C_1 in the Eq. (1) and Eq. (2) is 0.35 in which represented semi-empirical expressions from the experiments conducted by the authors. These are located within the first half of the equation which is a measure of the load-carrying capacity of the concrete strut of the lower path in the structural idealisation ($C_1 f_t b k_2 D$). The factor $\left[1 - 0.35 \frac{k_1 x}{k_2 D}\right]$ allows for experimental observation of the way the load capacity varied with $\cot \alpha$, where α is the inclination of the lower load path to the horizontal. As such, the first term is a semi-empirical expression for the capacity of the lower path – the strut fails when this capacity is reached. The second term represents the contribution of steel reinforcement to the shear strength of the beam. In this paper the second hand term will not be modified as the structural idealisation of the steel reinforcement is considered to be appropriately dealt with in this original manifestation.

3. EXPERIMENTAL PROGRAM

3.1 Test setup

In order to utilise previously published research (Kong *et al.* 1978, Tan et al, 2003 and Yang et al. 2006) for an in-depth comparison, an additional forty three deep beams with various opening sizes and locations were cast and tested to failure in this study. The overall dimensions of all deep beam specimens were 2400 mm × 600 mm × 110 mm thick, as detailed in Figure 2 (a) & (b). For specimens under the single-point loading shown in Figure 2(a), the shear span was 900mm, which resulted in a clear span to depth (L/D) ratio of 3 and a shear span to depth ratio (a/D) of 1.5. For those beams under two-point loading shown in Figure 2(b), L/D ratio and a/D equalled 3.0 and 1.0, respectively.

The size of openings were varied from 60mm×60mm to 210mm×210mm and the opening configurations for each specimen were detailed in Table 2 with details of geometric notations presented in Figure 3 (a) & (b). The existing test beams have the web opening ratios varied

$0.18 \leq a_1 \leq 0.38$ and $0.1 \leq a_2 \leq 0.4$. It presents the opening sizes are relatively larger and hence, there needs to be more details study on the openings ratios in the range $0.075 \leq a_1 \leq 0.3$ and $0.1 \leq a_2 \leq 0.4$.

Each beam consisted of two 20 mm diameter deformed reinforcement bars, with nominal yield stress of 500 MPa, in the longitudinal direction located close to the bottom of the beam. Each bar had a length of 2700mm and a 90 degree cog at each end with a vertical length 200mm to prevent end anchorage failure. The concrete was supplied by a local ready-mix company and the compressive concrete strengths for all specimens were mainly high strength varying from 63 to 91 MPa. It should be noted that four deep beam specimens (Group 8) comprised of concrete with a lower compressive strength of 34 MPa.

The test frame was designed to support a jack of 80 tonne capacity. Dial gauges were used to measure the vertical deflections of the beams at the midspan during testing (see Figure 4 (a) & (b)).

The deep beams were loaded in increments of approximately 10 kN at the beginning until an initial flexural crack was observed. The load increment was reduced to approximately 5kN afterwards. The load increment was further reduced to approximately 2kN after propagation of diagonal cracks. Upon approaching failure load, the load increment was made even smaller to 0.1 kN. At each load increment, crack patterns and deflections were recorded. The latter allowed the load-deflection history to be traced accurately.

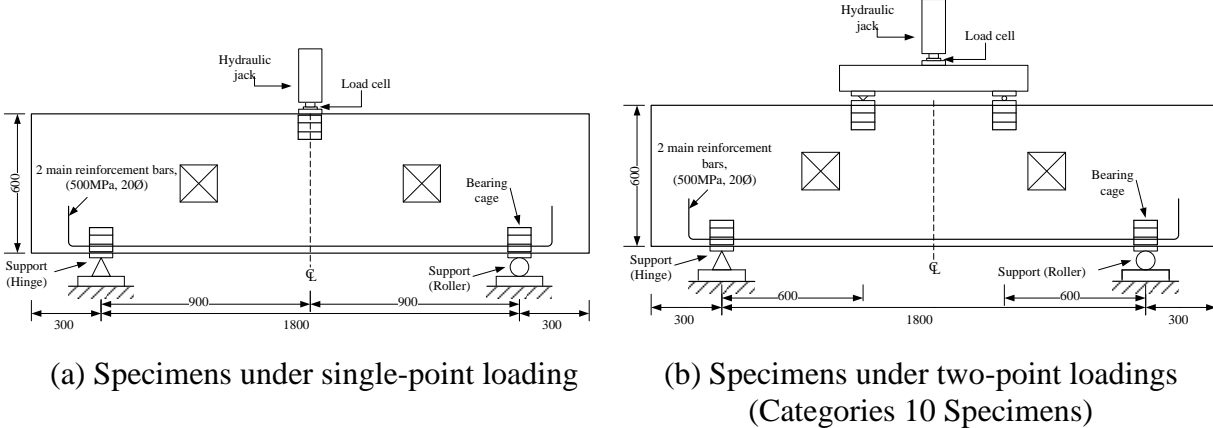


Figure 2. Details of deep beam specimens (dimensions in mm)

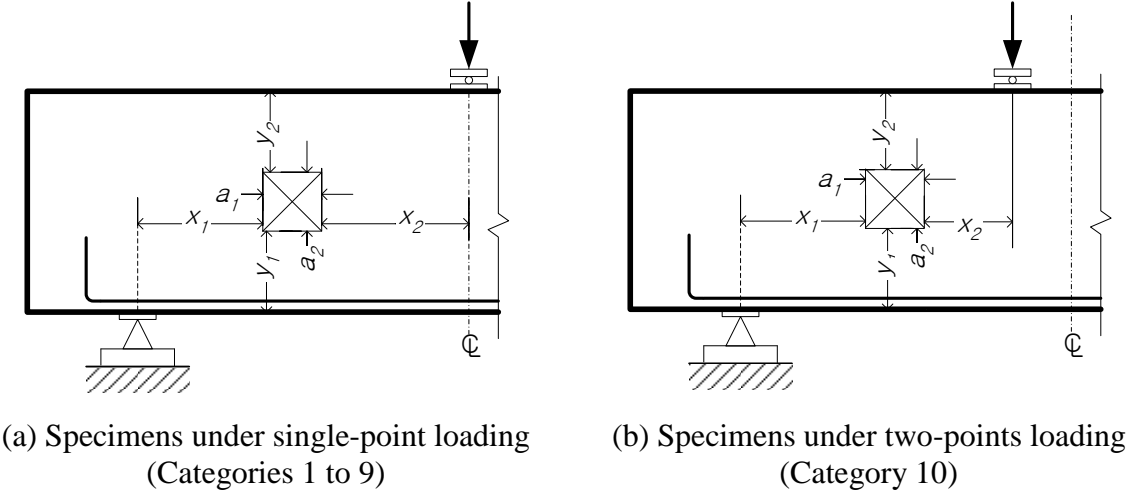


Figure 3. Notations for test specimens



(a) Side View



(b) Front view

Figure 4. Test setup

3.2 Test specimens

The beams were separated into three groups to ensure a variety of parameters relating to different behaviour characteristics was investigated. The varying parameters included concrete strengths, opening sizes, shapes, locations, and shear span-to-depth ratios. Dimensions of each deep beam specimen are detailed in Table 1 and in Figures 5 to 7.

3.2.1 Group 1

Group 1 specimens were divided into four Categories (Category 1, 2, 3 & 4) to observe the effect of location of a web opening on the high strength concrete (HSC) deep beams. There were four specimens cast for each category in this group. The web opening remained at a standard size of 60mm×60mm with its various positions. The varying parameters were:

- Category 1- the location of the web opening remained at mid-depth of the beam, but was moved sideways for each of the allocated test specimens (see Figure 5(a));
- Category 2- the location of the web opening remained at mid-depth of the beam but was moved up or down for each of the test specimens(see Figure 5(b));
- Category 3- the location of the web opening was positioned at different locations diagonally – parallel to the critical load path (see Figure 5(c));
- Category 4- the location of the web opening was positioned at different locations diagonally in the beam, but perpendicular to the critical shear load path (see Figure 5(d)).

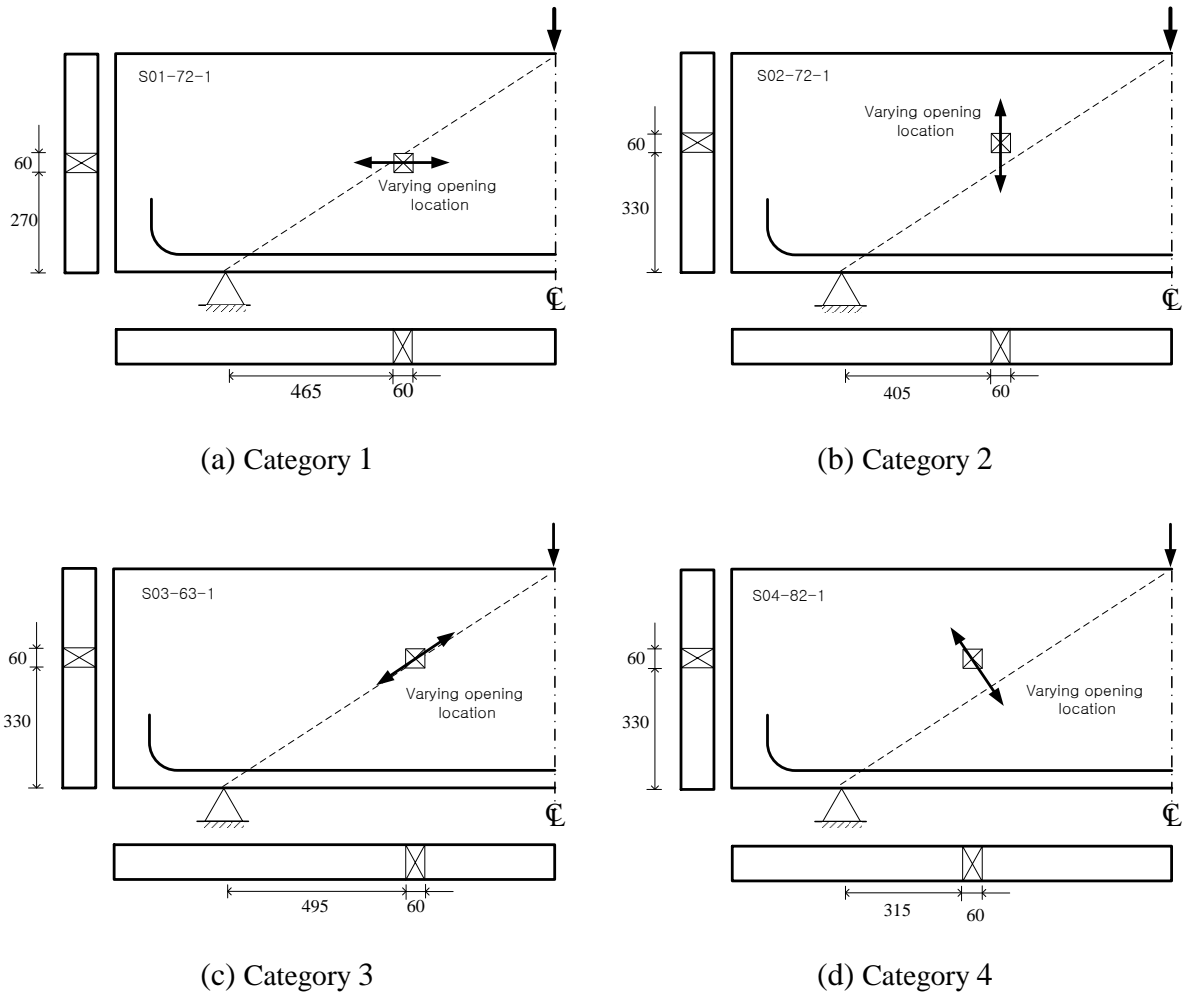
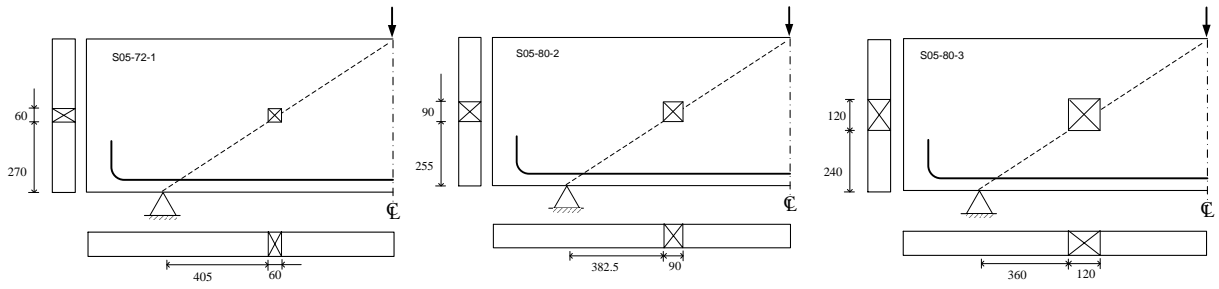


Figure 5. Group 1 test specimens (dimensions in mm)

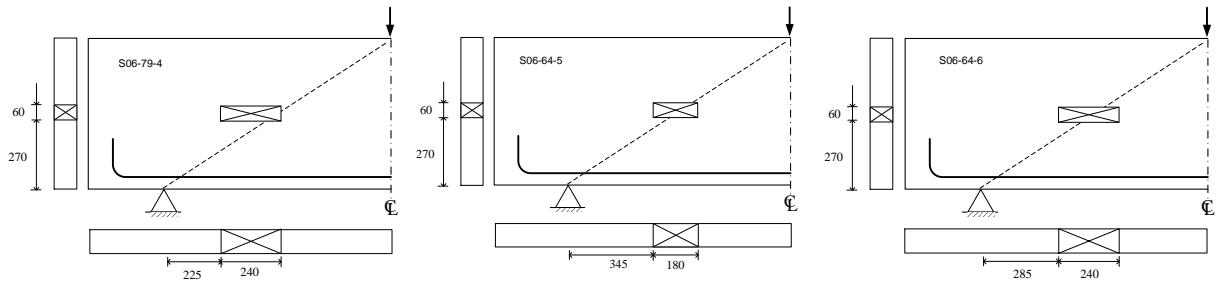
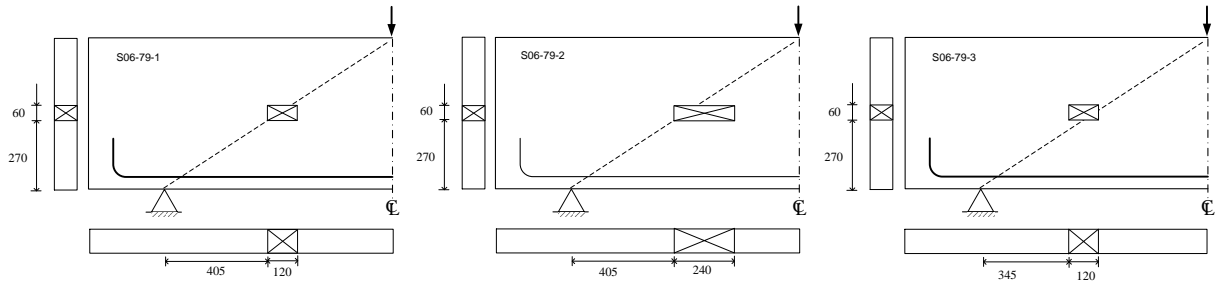
3.2.2 Group 2

Group 2 beams consisted of three Categories (Category 5, 6 & 7) to investigate the effect of web opening size and orientation on the behaviour of deep beams. The variables are:

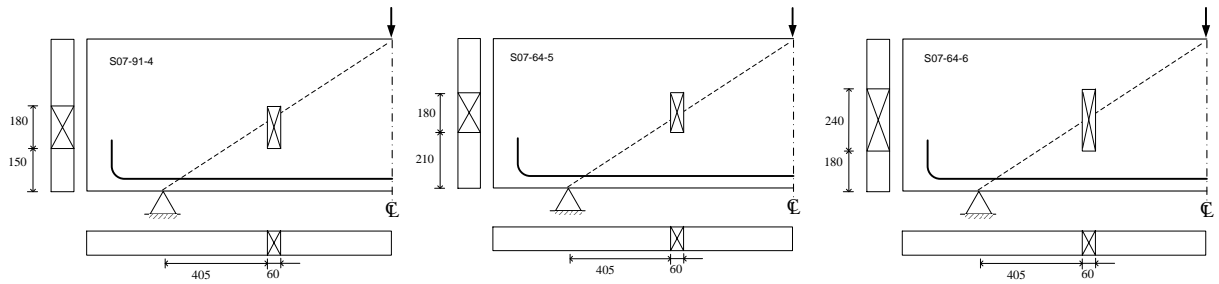
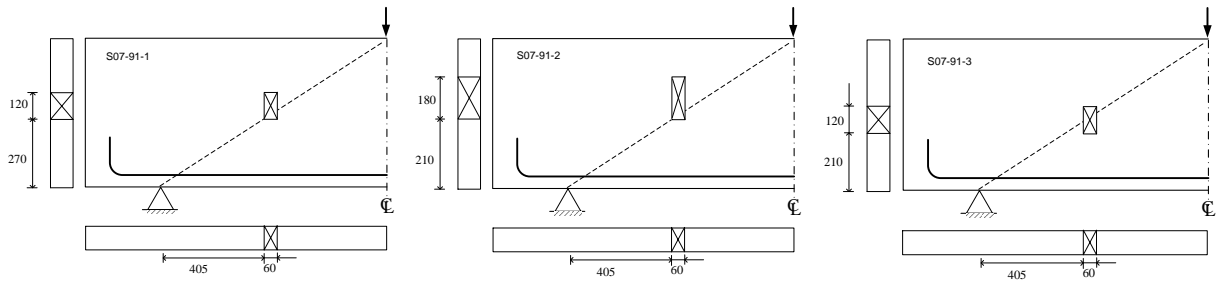
- Category 5- three HSC deep beams each with an increasing web opening size. The location of the centre of the opening remained at mid-depth of the beam (see Figure 6(a));
- Category 6- six HSC deep beams – the web opening was initially 120×60mm, with its location moving either left or right, or increasing in size to the left or right (see Figure 6(b));
- Category 7- six HSC deep beams – the web opening was initially 60×120mm, with its location moving either up or down, or increasing in size upwards or downwards(see Figure 6(c)).



(a) Category 5



(b) Category 6



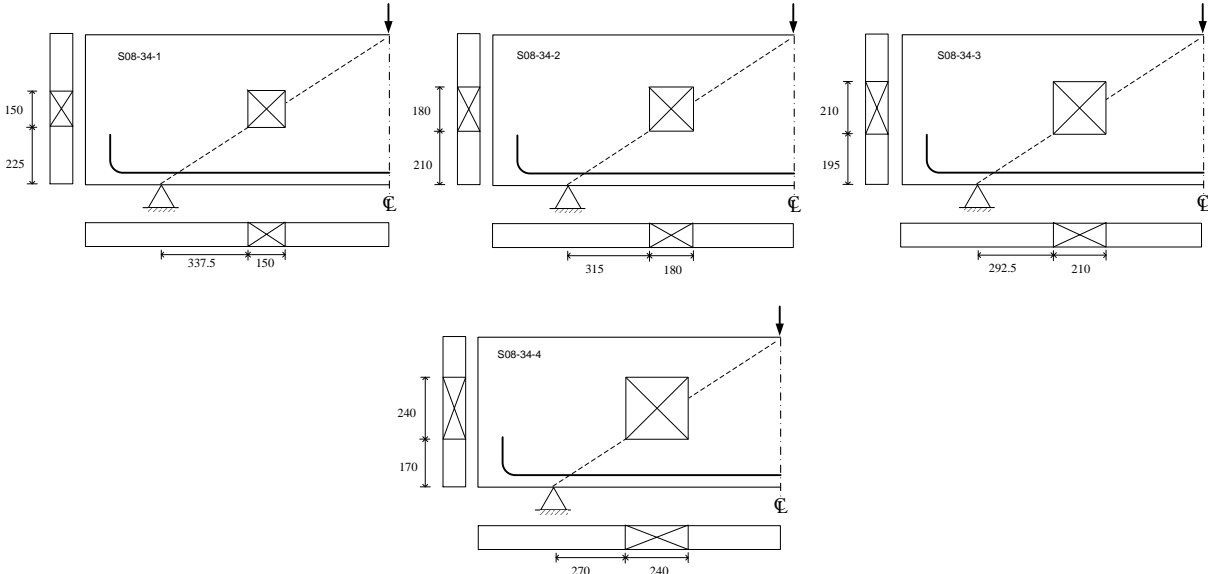
(c) Category 7

Figure 6. Group 2 test specimens (dimensions in mm)

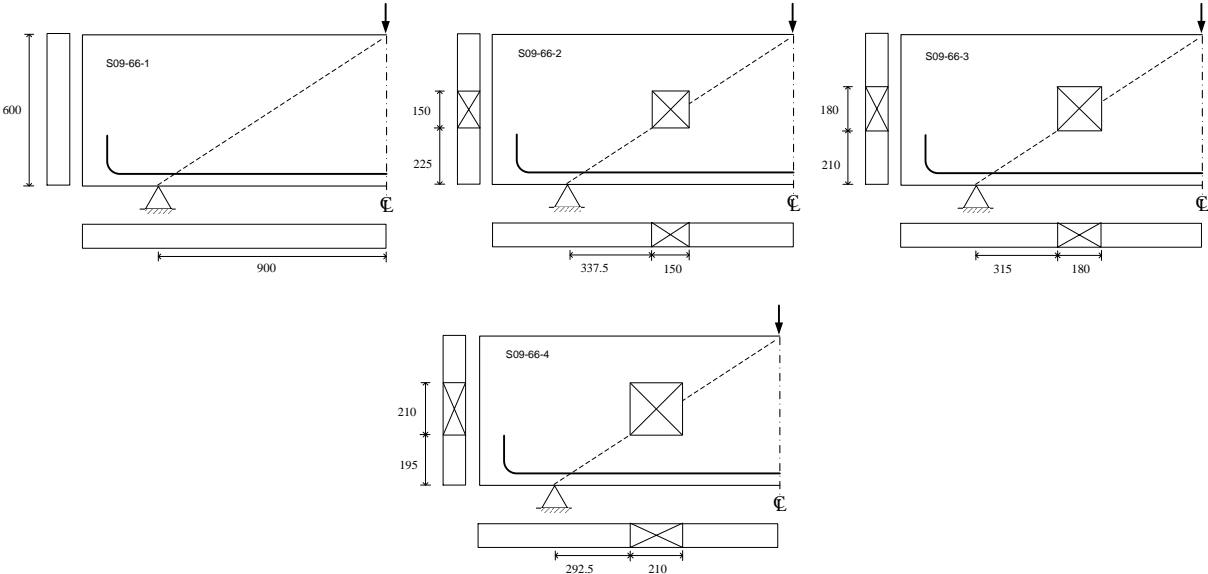
3.2.3 Group 3

Group 3 specimens also comprised of four categories (Category 8, 9 & 10), aimed at evaluating the effect of concrete strengths, opening sizes and shear span-to-depth ratios on beams with and without web openings. The variables were:

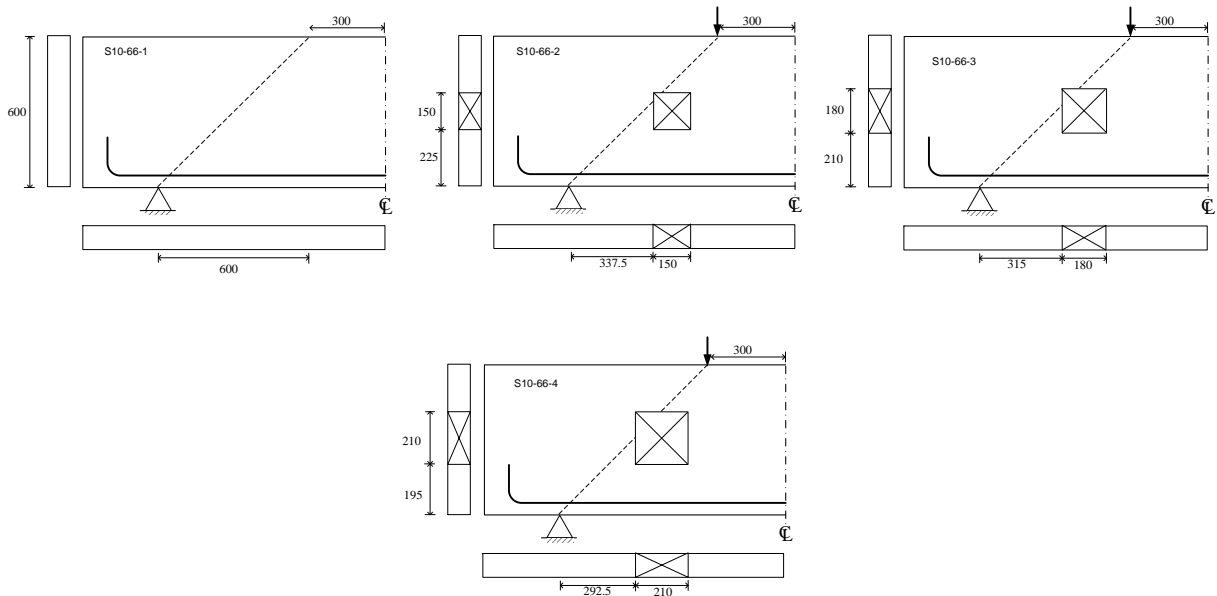
- Category 8- four normal strength concrete deep beams each with an increasing web opening size. The location of the centre of the opening remained at mid-depth of the beam. Shear span to depth ratio was 1.5. (see Figure 6(a));
- Category 9- four high strength concrete deep beams – one solid deep beam and three with an increasing web opening size. The location of the centre of the opening remained at mid-depth of the beam. Shear span to depth ratio was 1.5 (see Figure 6(b));
- Category 10- four deep beams with web opening configurations the same as Category 9 beams but the shear span to depth ratio decreased to 1.0 (see Figure 6(c)).



(a) Category 8



(b) Category 9



(c) Category 10

Figure 7. Group 3 test specimens (dimensions in mm)

4. RESULTS AND DISCUSSION

4.1 Crack patterns

Typical crack patterns for a sample of the deep beams tested are given in Figures 8 to 17. All of the beams exhibited crack patterns and failure modes that are consistent with the expected behaviour of simply supported deep beams with openings. In the majority of cases flexural type cracks were evident in initial stages. These crack developments ceased to propagate once shear cracks appeared near the edge of corners and near the load point and support conditions. Most specimens developed flexural cracks once loading reached approximately 30% of the ultimate strength. At 70-90% of the ultimate load, diagonal cracks generally developed around the corner of the web openings toward the supports and also under load points. These crack propagations formed in rapid manner when loading approach failure. Overall it seems openings played a major role in cracking behaviour, with more evidence of shear type cracking, whereas the beams with no openings (Figures 14 and 16) exhibit the more typical shear-flexure type cracking behaviour.



Figure 8. Failure crack patterns S03-63-1



Figure 9. Failure crack patterns S03-63-4



Figure 10. Failure crack patterns S05-72-1



Figure 11. Failure crack patterns S06-79-1



Figure 12. Failure crack patterns S07-64-5



Figure 13 Failure crack patterns S07-64-6



Figure 14. Failure crack patterns S09-66-1



Figure 15. Failure crack patterns S09-66-3

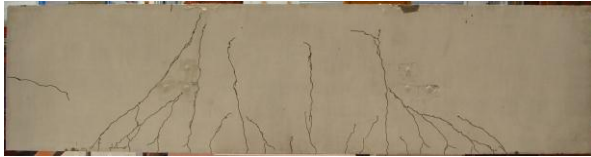


Figure 16. Failure crack patterns S10-66-2

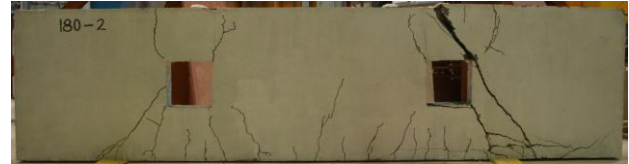


Figure 17. Failure crack patterns S10-66-3

4.2 Ultimate Strength Behaviour: Categories 1 and 2

Category 1 beams (along with S05-72-1 in Category 5) are designed to observe the relationship of a change in opening location in the horizontal direction. Table 3 presents the ultimate shear strength from the test results, V_{Exp} , which shows that as the opening moves toward the critical load path, the ultimate strength of the deep beam decreases. This becomes clearer in Figure 18, where the beam with opening on critical load path produce the lowest ultimate strength. The reduction in ultimate strength can be attributed to the decrease of the effective compressive area of the concrete.

Beams S01-72-2 S01-72-3 and S01-72-4 failed at approximately the same ultimate load, indicating that shear strength is relatively unaffected when the opening is way from the critical load path.

Also presented in Table 3 are the predicted strengths using Eqs. (2) and (3), $V_{Eq(2)}$ and $V_{Eq(3)}$. The predicted strengths are much lower than actual test results, and in fact are more than 50% less in most cases. Test results indicate that with increasing of k_l from 0.29 to 0.59 (ie. Opening tending towards critical path), the ultimate strength of the beam decreases by about 20%. This decrease appears much greater using prediction results. The differences between actual and predicted strengths using Eqs. (2) and (3) is also highlighted in Figure 20, with both predictions indicating significant ultimate strength decrease with an increase in k_l ratio. However, this trend not supported by the experimental results. Note that in testing, S05-72-1 had a lower ultimate strength than the other four specimens due to the location of the opening at the largest disturbance to the compressive strut.

Category 2 beams are designed to observe the relationship of a change in opening location in the vertical direction. Previous research suggests that as the opening moves away from the critical load path the strength of the beam will increase, this trend was also observed in the experimental results. It can be seen from Figure 19 that the strength of the beam decreases as the opening is moved to a lower position. The reason for this may be that by lowering the position of the opening, the effective depth of the neutral axis tends upwards, meaning there is more concrete in tension. The area gain in tension has a larger effect than the decrease of area in compression, resulting in a lower ultimate load. Figure 21 shows the ultimate shear load versus depth from opening to bottom (k_2). It can be seen from this figure that predictions of ultimate strength with Eqs. (2) and (3) increase as the web opening moves away from the soffit of the beam. The ratios of the increments of the predicted results are near uniform and thus conform to a linear relationship. Once again, the predicted strengths are much lower than actual test results. Therefore the ultimate strengths predicted by previous researchers are too conservative

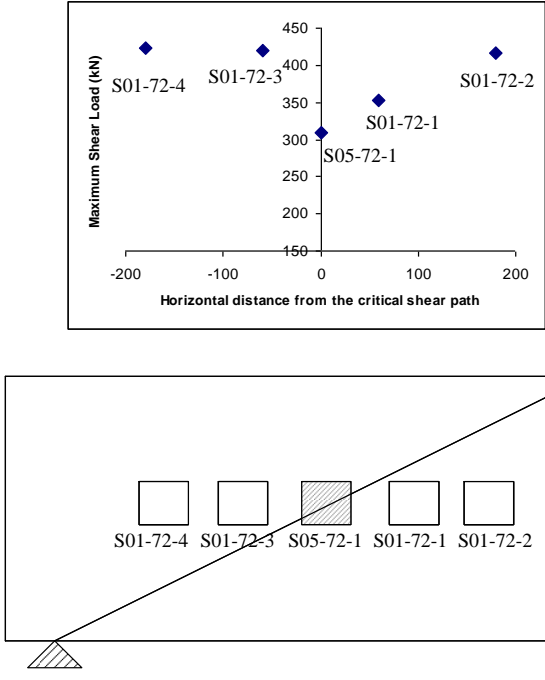


Figure 18 Horizontal Position of Opening versus Ultimate Load

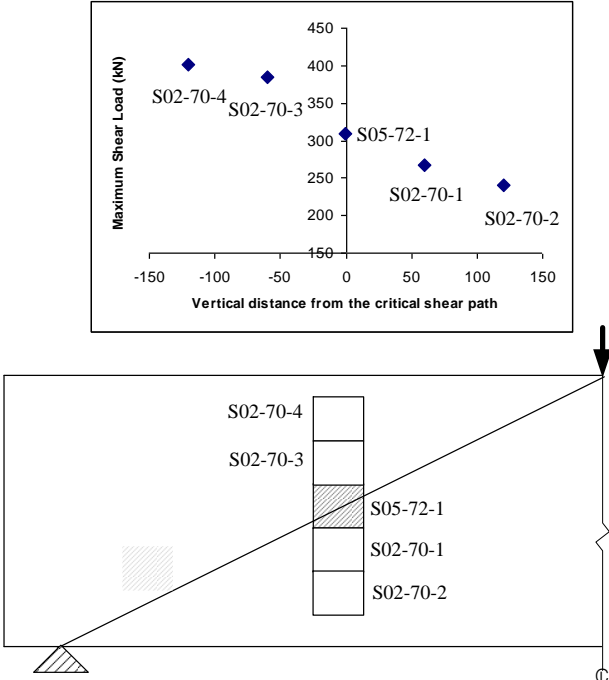


Figure 19 Vertical Position of Opening versus Ultimate Load

4.3 Ultimate Strength Behaviour: Categories 3 and 4

Category 3 represents the varying of both horizontal and vertical opening location ratios, k_1 and k_2 . Experimental results along with predictions are again presented in Table 3 and graphically in Figure 22. In general, the test results and the ultimate strength predictions increased with the increase of k_1 and k_2 . However the test ultimate strength of S03-63-2 illustrated an unexpected different behaviour with an ultimate strength lower than that of S03-63-1. This is possibly due to the shape of the strut and the reduction effect caused by the opening. The strut is actually representative of a bottle shape with the stress from the load area spread out along the diagonal load path. When the opening is located at the neck area of

the bottle shape strut, the reduction effect due to the opening is greater than when the opening is located proximate to neutral axis of the beam. The predicted ultimate load capacities using Eqs. (2) and (3) are again lower than experimental values, and increase as the web opening moves away from the soffit, even though the web opening is located close to the loading zone.

The test ultimate strengths of the Category 4 specimens are similar to each other when the openings were located above the critical zone as shown in Table 3 and indicated in Figure 23. However, the ultimate strengths decreased significantly when openings were located in the flexural zone. The conservative nature of both Eqs. (2) and (3) was evident for the high strength concrete deep beams tested. It should be noted that Eq (2) actually gives a negative result for the S04-82-4 implying zero strength as shown in Table 3. This highlights the need for a modified design equation to predict the maximum shear strength for such high strength concrete deep beams with openings located near the flexural zone.

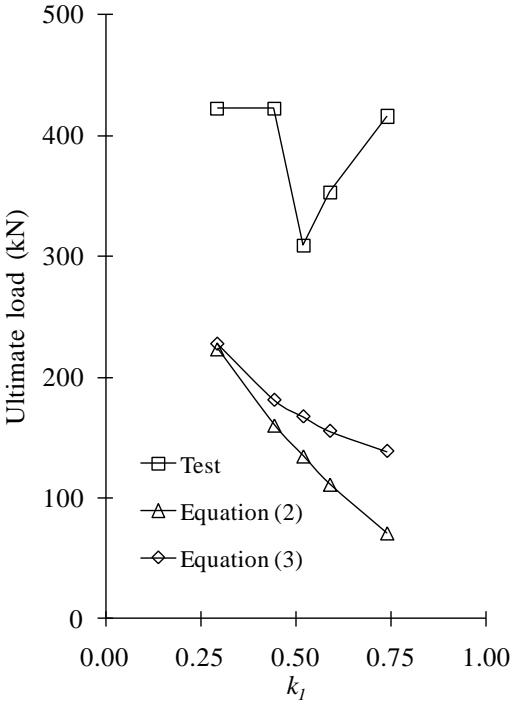


Figure 20. V versus k_1 - Category 1 specimens

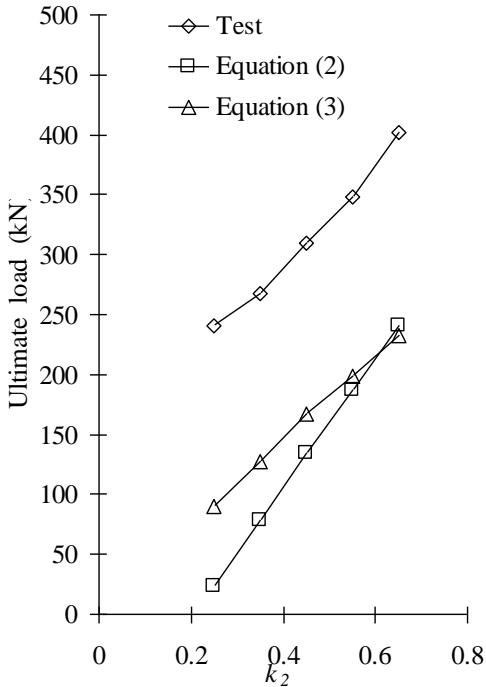


Figure 21. V versus k_2 - Category 2 specimens

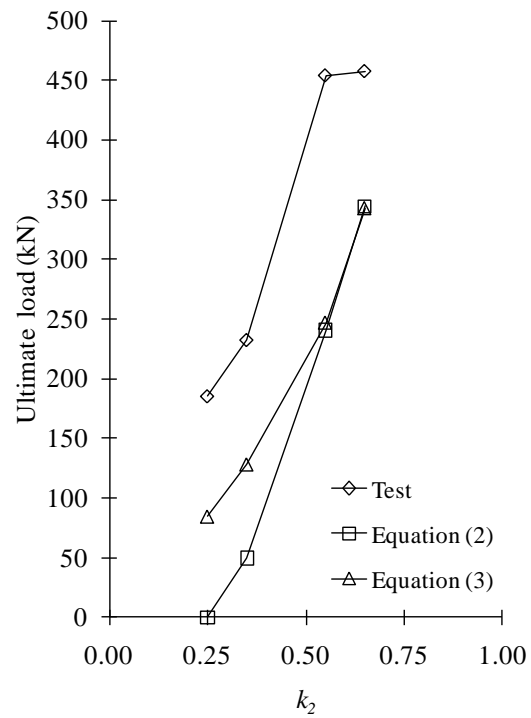
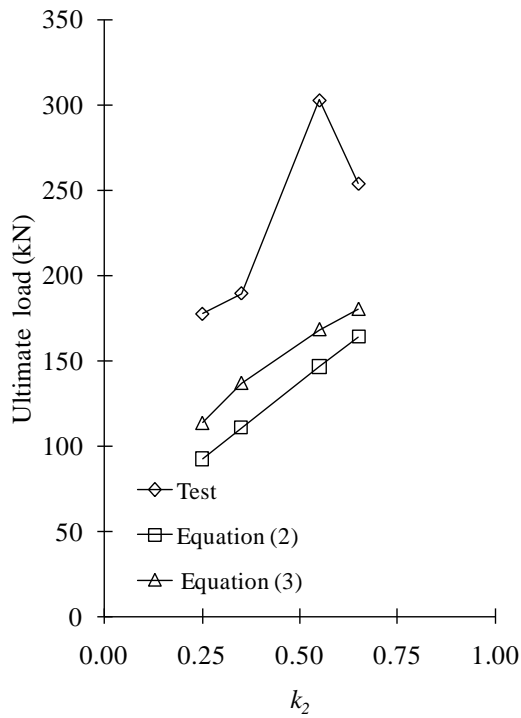


Figure 22. V versus k_2 - Category 3 specimens Figure 23. V versus k_2 - Category 4 specimens

4.4 Ultimate Strength Behaviour: Categories 6 and 7

Category 6 and 7 beams were tested to observe the effect of web opening size and orientation, where the web opening was elongated incrementally in different directions. Similar to the Category 2 beams, the ultimate shear loads in Category 6 were found to increase linearly with an increase in k_1 value. Also it was found that for Category 7 beams there was an increase of about 44 % in ultimate shear strength for an increase of k_2 from 0.25 to 0.45. Interestingly, in these categories, it was found that the equations gave a closer prediction of actual ultimate strength. It can be noted that opening sizes are larger than in previous categories resulting in much lower experimental ultimate strengths.

4.4 Ultimate Strength Behaviour: Categories 5, 8, 9 and 10

As can be seen in Table 3, as the web opening size increases a significant decrease in the ultimate strength occurs in all these categories. The ultimate loads achieved for the single point loaded deep beams (Category 9) were much lower when compared to the corresponding two-point loaded deep beams (Category 10). Thus a decrease in shear span ratio will lead to an increase in the ultimate strength. This effect was more pronounced when the compressive strength of the concrete was higher.

A further significant observation can be made between normal and high strength concrete deep beams using Table 3.. For the normal strength concrete deep beams of Category 8, an increase in the opening size from 150mm to 210mm led to a strength reduction of 17.8%. The increased size of the web opening was a more significant factor in high strength concrete deep beams where it was observed that an increase in the opening size from 150mm to 210mm led to a strength reduction of 34.4% and 70.0% for single point loaded beams (Category 9) and

double-point loaded beams (Category 10), respectively. For beams loaded at two points (Category 10), greater reduction in shear strength of the deep beams can be attributed to the influence the larger opening had on the shear path.

4.5 Overall Comparison study: predicted versus actual ultimate strengths

As highlighted in Table 2, the calculated ultimate strength using Eqs. (2) and (3) proposed by previous researchers were compared with the experimental test results of the 43 deep beams with and without web openings. Even though the proposed Eq. (2) gives a safe estimate of failure load for all beams with a mean (Predicted/Experimental) of 0.57 and standard deviation of 0.23, the result is quite conservative. Also for some predictions such as when the opening size increases and the opening approaches nearer to the bottom of the beam, Eq. (2) yields negative strength values which indicate zero capacity. The reason is that the empirical coefficients obtained from the previous research for normal strength or lightweight concrete are not valid for the high strength concrete deep beams with openings in this research. Hence the failure load predictions obtained from this method produce greater discrepancies.

On the other hand, Eq. (3) gives a more acceptable mean of 0.82 ratio, but a higher standard deviation of 0.33. There are a number of ratios that are greater than 1 for Groups 2 and 3 samples, suggesting that the equation overestimates the failure load, which could be unsafe. It is therefore evident that, even though Tan *et al.* (2003) have extensively investigated and proposed design equations for normal strength concrete deep beams, modifications are still required to produce a satisfactory design formula for high strength concrete deep beams, particularly when openings are located near critical shear paths.

The approach used in Eq. (3) utilises the more modern strut-and-tie method that accounts for the flow of forces around the openings. This method uses ratios of the forces in the upper and lower load paths, and as such is iterative and can be quite lengthy if web reinforcement is present. It can also be seen from the comparison results that the equation is conservative in describing the strength of beams with web openings located away from the critical shear path.

5. PROPOSED DESIGN EQUATION

Based on the above finding, the parameter of opening location and size λ_c can be expressed as a combination of the parameters of the horizontal and vertical opening location and size change.

λ_c , by Kong (1990) was

$$\lambda_c = (1 - m) \quad (5a)$$

where m is the ratio of strength reduction of opening location and size (ψ_x/ψ_y) multiplied by the shear span to depth ratio (x/D). Re-arranging Eq.(5a) leads to

$$\lambda_c = 1 - \frac{\psi_x x}{\psi_y D} \quad (5b)$$

Kong (1990) proposed that the strength reduction parameter due to the existence of opening, λ_c , is to represent typical diagonal mode of failure generally termed as shear-proper, shear-flexure and shear-compression, and the failure is mainly related to the shear-span to depth ratio (x/D). Kong (1990) also proposed that eccentricities of the opening in horizontal and

vertical dimensions can be combined with the effect of size of opening as well as location of openings. Therefore ψ_x can be expressed as

$$\psi_x = 1 - \frac{e_x}{x} \quad (5c)$$

in where the eccentricity of opening in horizontal dimension, $e_x = 1 - (2k_1 - t_3 a_1)x$.

Similarly,

$$\psi_y = 1 - \frac{e_y}{D} \quad (5d)$$

where the eccentricity of opening in vertical dimension, $e_y = 1 - (2k_2 + t_4 a_2)D$.

Therefore, substituting Eqs. (5c) and (5d) into Eq. (5b) leads to

$$\lambda_c = \left(1 - t_2 \left(\frac{2k_1 - t_3 a_1}{2k_2 + t_4 a_2} \right) \right) \frac{x}{D} \quad (5e)$$

where t_2 , t_3 and t_4 are the coefficients of the parameters, k_1 , k_2 , a_1 and a_2 are shown in Eq. (5e). The expression in bracket in Eq. (5e) is the combination of eccentricity of the opening centre to the beam centre in the horizontal and vertical directions.

The ultimate strength related to steel is adopted from Eq. (2). Therefore, V_s is

$$V_s = C_2 \sum \lambda \frac{A y_1}{D} \sin^2 \theta \quad (5f)$$

The coefficients of the parameters (C , t_2 , t_3 and t_4) are obtained by linear analysis based on least square method using numerical parametric study results for best fit (Yoo, 2011). This yields for Rigid zone, $C_1 = 1.1$, $t_2 = 0.2$, $t_3 = -0.5$ and $t_4 = 0.3$ and for Flexural zone, $C_1 = 1.2$, $t_2 = 0.15$, $t_3 = -0.1$ and $t_4 = 0.9$.

Therefore the proposed design equation for high strength concrete deep beams with web openings is expressed as

$$V_{Flex} = 1.2 \left(1 - 0.15 \cdot \left(\frac{(2k_1 + 0.10a_1)}{(2k_2 + 0.90a_2)} \right) \left(\frac{x}{D} \right) \right) f_t b k_2 D + C_2 \sum \lambda \frac{A y_1}{D} \sin^2 \theta \quad (6)$$

for opening located in Flexural zone, and

$$V_{Rigid} = 1.1 \left(1 - 0.2 \cdot \left(\frac{(k_1 + 0.25a_1)}{(k_2 + 0.15a_2)} \right) \left(\frac{x}{D} \right) \right) f_t b k_2 D + C_2 \sum \lambda \frac{A y_1}{D} \sin^2 \theta \quad (7)$$

for opening located in Rigid zone

5.1 Verification of proposed equation

To verify the proposed design equation, a comparison of proposed equations and other existing equations is made utilising the experiment results presented in Table 3. Table 3 shows the details of the experimental results (V_{Exp}) and the ultimate strength predictions due

to the proposed equations ($V_{Proposed}$), Eq. (2) ($V_{Eq.(2)}$) and Eq. (3) ($V_{Eq.(3)}$). The ratios $V_{Proposed}/V_{Exp}$, $V_{Eq.(2)}/V_{Exp}$ and $V_{Eq.(3)}/V_{Exp}$ are also presented in the table. The average values of the three ratios are shown to be 0.81, 0.57 and 0.82, respectively and the corresponding standard deviations are 0.31, 0.23 and 0.33, respectively. The proposed equations give a safe estimate of failure load. Even though Eq. (3) has a better mean value, the standard deviation is slightly higher than the proposed design equations.

Again less accurate predictions are found for deep beam specimens with web opening located closer to the beam soffit and/or centre. However, these specimens can be neglected due to unpractical location or size of the opening. The modification is acceptable because of the increased strength obtained in the testing and the application of the capacity reduction assures that all the experimental test results fall well below the predicted design load.

Further comparisons of the proposed equations with test results of Yang et al. (2006) demonstrate the advantage and benefit of the proposed equations. Yang et al. (2006)'s experiment was focused on high strength concrete deep beams with web openings but without web reinforcement. This is similar to the experimental conditions of the present work and hence, this comparison is valid. In addition, Yang et al.'s (2006) work was to investigate the effect of main longitudinal steel and shear span to depth ratio when web opening changes. The impact of the change in opening size and location was not evaluated in detail. The present study thus offers more insight into this area to further advance the fundamental understanding provided by the existing research.

As shown in Table 4, the proposed equations are able to make better ultimate strength predictions than the other existing equations, based on published experimental results of Yang et al. (2006). The mean ratio of $V_{Proposed}/V_{Exp}$ is 1.00 and the standard deviation is 0.18. Whereas the mean ratios of $V_{Eq.(2)}/V_{Exp}$ and $V_{Eq.(3)}/V_{Exp}$ are 0.84 and 0.93, respectively with standard deviations of 0.15 and 0.21, respectively. Overall Eq. (2) and Eq. (3) predict the experimental ultimate strength successfully. However, the proposed equation showed better accuracy on the data collected from literature.

6. CONCLUSION

An experimental program has been undertaken to investigate the applicability of current design methods for concrete deep beams with various web opening configurations. A comparative study indicates that the currently available design methods proposed by previous researchers are inadequate in their strength predictions, particularly for deep beams with high strength concrete. In such cases the formulae can yield conservative and at times underestimate strengths. They can also produce negative strength values which indicate zero load-bearing capacity, which was found to be incorrect in this experimental evaluation. Further, it was generally found that the accuracy of both proposed design procedures decreased as the distance from the critical load path increased.

Consequently the study found that the concrete deep beams have significantly reduced strengths with various web opening sizes and its locations. The current design methods do not adequately account for these variations. In view of the significant shortcomings, there is a need to amend current design formulae. The special feature of the formulae is its applicability to both normal and high strength concrete deep beams with various web openings. It also caters for the effect of opening sizes and various locations. Comparisons with test data and previous test results confirmed that the new formula is accurate and reliable.

The presented results give a general overview of trends. More detailed analysis is required before a reliable prediction formula can be established. This may include various support conditions, shear span to depth ratios and varying web steel ratios and orientation.

REFERENCES

- ACI318-09. 2009. Building Code Requirements for Structural Plain Concrete. *American Concrete Institute*, Detroit.
- AS3600-2009. 2009. Concrete Structures”, *Standards Australia*. Sydney, Australia, 2009.
- Ashour, A.F. & Yang, K.-H. 2008. ‘Application of plasticity theory to reinforced concrete deep beams: a review’, *Magazine of Concrete Research*, **60**(9):657-664.
- Ashour, A.F. & Rishi, G. 2000. Tests of reinforced concrete continuous deep beams with web openings, *ACI Structural Journal* **97**(5): 418-426.
- Eun, H.C, Lee, Y.H., Chung H.S. and Yang, K.H. 2006. On the Shear Strength of Reinforced Concrete Deep Beam with Web Opening. *The Structural Design of Tall and Special Buildings* DOI: 10.1002/tal.306.
- Guan, H., & Doh, J. 2007. Development of Strut-and-Tie Models in Deep Beams with Web Openings. *Advances in Structural Engineering* **10**(6): 697-711.
- Kong, F.K., Robins, P.J., & Cole, D.F. 1970. Web Reinforcement Effects on Deep Beams. *ACI Journal* **67**(12): 1010-1017.
- Kong, F.K. & Sharp, G.R. 1973. Shear strength of lightweight reinforced concrete deep beams with web openings. *The Structural Engineer* **51**(8): 267-275.
- Kong, F.K. & Sharp, G.R. 1977. Structural idealization for deep beams with web openings. *Magazine of Concrete Research*, **29**(99): 81-91.
- Kong, F. K., Sharp, G.R., Appleton, S.C., Beaumont, C.J., & Kubik, L.A. 1978. Structural idealization for deep beams with web openings: further evidence. *Magazine of Concrete Research* **30**(103): 89-95.
- Kong, F. K. 1990. Reinforced Concrete Deep Beams. New York: Routledge.
- Leong, C.L. & Tan, K. H. 2003. Proposed Revision on CIRIA Design Equation for Normal and High Strength Concrete Deep Beams. *Magazine of Concrete Research* **55**: 267-278.
- Mansur M.A. & Alwis W.A.M. 1984, Reinforced fibre concrete deep beams with web openings, *International Journal of Cement Composites and Lightweight Concrete* **6**(4): 263-271.
- Maxwell, B.S. & Breen, J.E. 2000. Experimental evaluation of strut-and-tie model applied to deep beam with opening, *ACI Structural Journal* **97**(1): 142-149.
- Ray S.P. 1991, Deep beams with web openings. *Reinforced Concrete Deep Beams* 60-94.
- Tan, K. H. & Mansur, M. A. 1992, Partial Prestressing in Concrete Corbels and Deep Beams. *ACI Structural Journal* **89**: 251-262.
- Tan, K.H, Tong, K, & Tang, C.Y. 1997. Effect of web reinforcement on high strength concrete deep beams. *ACI Structural Journal* **94**(5): 572-82.
- Tan, K. H., Kong, F. K., Teng, S. & Guan, L. 1995. High-Strength Concrete Deep Beams with Effective Span and Shear Span Variations. *ACI Structural Journal* **92**: 1-11.
- Tan, K. H., Lu, H.Y. & Teng, S. 1999. Size Effect in Large Prestressed Concrete Deep Beams. *ACI Structural Journal* **96**: 937-946.
- Tan, K.H., Tong, K., & Tang, C.Y. 2003. Consistent strut-and-tie modelling of deep beams with web openings. *Magazine of Concrete Research* **55**(1): 65-75.
- Yang, K.H., Eun, H.C., & Chung, H.S. 2003. Shear characteristics of high-strength concrete deep beams without shear reinforcement. *Engineering Structures* **25**(8): 1343-52.

- Yang, K.H., Eun, H.C., & Chung, H.S. 2006. The influence of web openings on the structural behavior of reinforced high-strength concrete deep beams. *Engineering Structures* **28**(13): 1825-1834.
- Yang, K.H., Chung, H.S. & Ashour, A.F. 2007. Influence of inclined web reinforcement on reinforced concrete deep beams with openings, *ACI Structural Journal* **104**(5): 580-589.
- Yang, K. H. & Ashour A. F. 2008. Code modelling of reinforced concrete deep beams. *Magazine of Concrete Research*, 2008, **60**(6): 441–454.
- Yoo. T.M., 2011. Strength and behaviour of high strength concrete deep beam with web opening, *PhD Thesis*, Griffith University.

NOTATION

a	shear span measured between concentrated load and support point
a_1	width of opening
a_2	depth of opening
a_1	ratio of width of opening to the shear span
a_2	ratio of depth of opening to the depth of the beam
A_c	area of concrete strut
A_s	cross section of main reinforcement bars
A_{st}	area of an individual web bar or longitudinal bar
A_{str}	cross sectional area of diagonal strut
A_{suh}	area of single horizontal web reinforcement
A_w	area of web reinforcement
b	breadth (thickness) of beam
C_1	empirical coefficient 1.4 , 1.35 and 1.1 for normal, lightweight concrete and high strength concrete respectively
C_2	empirical coefficient 300N/mm^2 and 130N/mm^2 for deformed and plain round bars respectively
d	effective depth of the beam
d_w	distance from the beam top to the intersection of web reinforcement with the diagonal strut
D	overall Depth of the Beam
f'_c	characteristic compressive cylinder strength of concrete at 28 days
f_{ct}	cylinder-splitting tensile strength of concrete
f_t	combined tensile strength of concrete and steel
f_{yw}	yield strength of web reinforcement
h	overall height of deep beam (= D)
k_1	ratio of width of bottom corner of the opening to the shear span
k_2	ratio of height of top corner of the opening to the height of the beam
l_a	depth of bottom nodal zone
l_b	width of support bearing plate
L	simple span of the beam
Q_{ult}	ultimate shear strength (Kong and Sharp 1977)
t_1, t_2, t_3, t_4	coefficients of the geometric parameters (Yoo, 2011)
V_n	ultimate shear strength (Tan <i>et al.</i> 2003)
V_{Flex}	proposed design equation for high strength concrete deep beams with web openings where opening located in flexural zone
V_{Rigid}	proposed design equation for high strength concrete deep beams with web openings where opening located in rigid zone
V_s	ultimate strength related to steel
w	total load on beam
x	clear-shear span distance
x_1	horizontal distance measured from the centre of the corner of support to the nearest corner of the opening
x_2	horizontal distance measured from the centre of the corner of support to the distant corner of the opening
x_e	clear shear span length
y	depth at which a typical bar intersects the potential critical diagonal crack, which forms approximately along the line joining the loading and reaction points

y_1	depth at which a typical bar intersects a potential critical diagonal crack in a deep beam with openings
y_2	width at which a typical bar intersects a potential critical diagonal crack in a deep beam with openings
θ_s	angle between the longitudinal tension reinforcement and the diagonal strut
θ_w	angle between the web reinforcement and the axis of beams at the intersection of the reinforcement and diagonal strut
α	angle of intersection between a typical bar and the potential critical diagonal crack described in the definition of y above
α_1	angle of intersection between a typical bar and a potential critical diagonal crack in a deep beam with openings
λ	empirical coefficient, equal to 1.5 for web bars and 1.0 for main longitudinal bars
ϕ	strength reduction factor

Table 1 Summary of the simply supported deep beam tests with web openings and variables used

Researcher	Concrete Strength (f'_c) MPa	Number of test specimen	Shear span to depth ratio (a/D)	Opening size ratio		Opening location ratio	
				Horizontal a_1	Vertical a_2	Horizontal k_1	Vertical k_2
Kong & Sharp (1973)	29.2-37.2	24	0.25, 0.4	0.25-0.5	0.1-0.4	0.63-1.0	0.12-0.8
Kong & Sharp (1977)	30.2-38.9	34	0.2, 0.3	0.3-1.5	0.2	0.3-1.3	0.13-0.67
Kong et al. (1978)	36.8-46.2	17	0.28, 0.3	0.3-1.0	0.2, 0.3	0.3-1.0	0.13-0.67
Ashour & Rishi (2000)	20.8-29.8	16	0.9	0.18, 0.38	0.2, 0.38	0.2, 0.3	0.3, 0.4
Maxwell & Breen (2000)	27.7-28.8	4	1.0	0.3	0.3	0.1	0.1
Yang et. al (2006)	24-80	32	0.5-1.5	0.25, 0.5	0.1-0.3	0.2-0.4	0.25-0.38

Table 2 Web opening configuration and concrete strength

	Specimens	f_c (MPa)	x_1 (mm)	x_2 (mm)	y_1 (mm)	y_2 (mm)	a_1 (mm)	a_2 (mm)	k_1	k_2	
Group 1	Category 1	S01-72-1	72	465	375	270	270	60	60	0.59	0.45
		S01-72-2		585	255	270	270	60	60	0.74	0.45
		S01-72-3		345	495	270	270	60	60	0.44	0.45
		S01-72-4		225	615	270	270	60	60	0.29	0.45
	Category 2	S02-70-1	70	405	435	330	210	60	60	0.52	0.55
		S02-70-2		405	435	390	150	60	60	0.52	0.65
		S02-70-3		405	435	210	330	60	60	0.52	0.35
		S02-70-4		405	435	150	390	60	60	0.52	0.25
	Category 3	S03-63-1	63	495	345	330	210	60	60	0.63	0.55
		S03-63-2		585	255	390	150	60	60	0.74	0.65
		S03-63-3		315	525	210	330	60	60	0.41	0.35
		S03-63-4		225	615	150	390	60	60	0.29	0.25
	Category 4	S04-82-1	82	315	525	330	210	60	60	0.41	0.55
		S04-82-2		225	615	390	150	60	60	0.29	0.65
		S04-82-3		495	345	210	330	60	60	0.63	0.35
		S04-82-4		585	255	150	390	60	60	0.74	0.25
Group 2	Category 5	S05-72-1	72	405	435	270	270	60	60	0.52	0.45
		S05-80-2	80	382.5	427.5	255	255	90	90	0.53	0.43
		S05-80-3		360	420	240	240	120	120	0.54	0.40
	Category 6	S06-79-1	79	405	375	270	270	120	60	0.59	0.45
		S06-79-2		405	255	270	270	240	60	0.74	0.45
		S06-79-3		345	435	270	270	120	60	0.52	0.45
		S06-79-4		225	435	270	270	240	60	0.52	0.45
		S06-64-5	64	345	375	270	270	180	60	0.59	0.45
		S06-64-6		285	315	270	270	240	60	0.59	0.45
	Category 7	S07-91-1	91	405	435	270	210	60	120	0.52	0.45
		S07-91-2		405	435	270	150	60	180	0.52	0.45
		S07-91-3		405	435	210	270	60	120	0.52	0.35
S07-91-4		405		435	150	270	60	180	0.52	0.25	
S07-64-5		64	405	435	210	210	60	180	0.52	0.35	
S07-64-6			405	435	180	180	60	240	0.52	0.30	
Group 3	Category 8	S08-34-1	34	337.5	412.5	225	225	150	150	0.55	0.38
		S08-34-2		315	405	210	210	180	180	0.56	0.35
		S08-34-3		292.5	397.5	195	195	210	210	0.57	0.33
		S08-34-4		270	390	170	170	240	240	0.58	0.28
	Category 9	S09-66-1	66	900	N/A	600	600	N/A	N/A	N/A	N/A
		S09-66-2		337.5	412.5	225	225	150	150	0.55	0.38
		S09-66-3		315	405	210	210	180	180	0.56	0.35
		S09-66-4		292.5	397.5	195	195	210	210	0.57	0.33
	Category 10	S10-66-1	66	600	N/A	600	600	N/A	N/A	N/A	N/A
		S10-66-2		337.5	112.5	225	225	150	150	0.88	0.38
		S10-66-3		315	105	210	210	180	180	0.89	0.35
		S10-66-4		292.5	97.5	195	195	210	210	0.91	0.33

Table 3 Comparison of predicted ultimate strengths by proposed equations, Eq. (2) and Eq. (3) utilising experimental results

Specimens	V_{Exp}	$V_{Proposed}$	$\frac{V_{Proposed}}{V_{Exp}}$	$V_{Eq(2)}$	$\frac{V_{Eq(2)}}{V_{Exp}}$	$V_{Eq(3)}$	$\frac{V_{Eq(3)}}{V_{Exp}}$
S01-72-1	352.8	157.7	0.45	110.9	0.31	155.0	0.44
S01-72-2	415.8	135.5	0.33	70.5	0.17	138.4	0.33
S01-72-3	422.4	166.6	0.39	160.0	0.38	180.8	0.43
S01-72-4	422.2	214.4	0.51	223.2	0.53	227.4	0.54
S02-70-1	347.7	193.1	0.56	187.5	0.54	198.9	0.57
S02-70-2	401.8	237.7	0.59	240.5	0.60	232.8	0.58
S02-70-3	267.9	121.3	0.45	77.8	0.29	127.5	0.48
S02-70-4	240.5	73.9	0.31	23.6	0.10	89.7	0.37
S03-63-1	303.1	189.0	0.62	146.7	0.48	168.5	0.56
S03-63-2	254.1	213.5	0.84	164.3	0.65	180.4	0.71
S03-63-3	189.7	139.4	0.73	111.0	0.59	137.1	0.72
S03-63-4	177.6	114.0	0.64	92.7	0.52	113.6	0.64
S04-82-1	454.2	234.3	0.52	240.6	0.53	246.7	0.54
S04-82-2	457.8	316.7	0.69	344.3	0.75	342.4	0.75
S04-82-3	232.3	111.2	0.48	49.3	0.21	128.0	0.55
S04-82-4	185.1	54.7	0.30	N/A*	N/A*	84.4	0.46
S05-72-1	309.1	172.1	0.56	134.3	0.43	167.0	0.54
S05-80-2	193.2	165.2	0.86	121.1	0.63	165.9	0.86
S05-80-3	112.8	152.2	1.35	103.7	0.92	155.0	1.37
S06-79-1	166.8	163.2	0.98	114.3	0.69	164.3	0.99
S06-79-2	122.6	140.1	1.14	72.5	0.59	147.6	1.20
S06-79-3	174.4	164.6	0.94	129.3	0.74	155.3	0.89
S06-79-4	122.8	138.6	1.13	129.3	1.05	155.3	1.27
S06-64-5	146.1	163.0	1.12	114.3	0.78	164.3	1.12
S06-64-6	138.2	162.7	1.18	114.3	0.83	164.3	1.19
S07-91-1	306.6	162.1	0.53	144.5	0.47	190.1	0.62
S07-91-2	157.9	163.6	1.04	144.5	0.91	190.1	1.20
S07-91-3	135.2	120.4	0.89	75.9	0.56	120.5	0.89
S07-91-4	111.8	78.0	0.70	23.4	0.21	84.3	0.75
S07-64-5	109.8	140.0	1.27	83.8	0.76	149.4	1.36
S07-64-6	81.4	116.8	1.44	53.6	0.66	128.5	1.58
S08-34-1	88.1	103.5	1.18	69.2	0.79	82.9	0.94
S08-34-2	87.0	93.8	1.08	56.5	0.65	75.9	0.87
S08-34-3	79.5	65.7	0.83	44.1	0.56	68.9	0.87
S08-34-4	72.4	69.8	0.96	25.3	0.35	58.1	0.80
S09-66-1	489.5	270.2	0.55	248.1	0.51	227.2	0.46
S09-66-2	125.6	130.2	1.04	82.0	0.65	128.6	1.02
S09-66-3	93.2	118.5	1.27	66.2	0.71	118.9	1.28
S09-66-4	78.9	80.9	1.02	50.7	0.64	109.2	1.38
S10-66-1	657.6	673.5	1.02	701.6	1.07	569.4	0.87
S10-66-2	583.1	260.1	0.45	164.0	0.28	256.7	0.44
S10-66-3	334.5	236.8	0.71	132.4	0.40	237.3	0.71
S10-66-4	174.4	214.2	1.23	101.3	0.58	218.0	1.25
Average			0.81		0.57		0.82
Standard Deviation			0.31		0.23		0.33

* The negative strength values which indicate zero-bearing capacity

Table 4 Comparison of predicted ultimate strengths by proposed equations, Eq. (2) and Eq. (3) utilising Yang et al. (2006)'s experiment results

Specimens	V_{Exp}	$V_{proposed}$	$\frac{V_{Proposed}}{V_{Exp}}$	$V_{Eq(2)}$	$\frac{V_{Eq(2)}}{V_{Exp}}$	$V_{Eq(3)}$	$\frac{V_{Eq(3)}}{V_{Exp}}$
H5NN	684.0	559.5	0.82	624.9	0.91	592.5	0.87
H5F1	466.3	342.6	0.73	341.5	0.73	302.4	0.65
H5F2	347.9	310.9	0.89	304.6	0.88	269.7	0.78
H5F3	288.6	276.5	0.96	264.8	0.92	235.3	0.82
H5T3	336.6	306.3	0.91	302.3	0.90	267.8	0.80
H5S3	235.7	260.1	1.10	243.9	1.03	220.1	0.93
H10NN	476.0	445.9	0.94	464.2	0.98	407.1	0.86
H10F1	224.8	225.2	1.00	182.1	0.81	192.7	0.86
H10F2	183.8	196.5	1.07	145.9	0.79	171.5	0.93
H10F3	144.1	167.9	1.16	109.6	0.76	149.8	1.04
H10T3	163.2	193.2	1.18	150.1	0.92	167.2	1.02
H10S3	129.5	155.9	1.20	88.5	0.68	141.8	1.09
UH5NN	823.0	641.4	0.78	722.1	0.88	781.8	0.95
UH5F1	514.5	382.4	0.74	381.1	0.74	366.7	0.71
UH5F2	419.4	346.3	0.83	338.5	0.81	325.6	0.78
UH5F3	339.1	307.4	0.91	293.1	0.86	283.5	0.84
UHFT3	394.9	338.0	0.86	333.0	0.84	320.7	0.81
UH5S3	331.2	290.6	0.88	270.7	0.82	266.5	0.80
UH7NN	744.0	591.4	0.79	648.9	0.87	655.3	0.88
UH7F3	263.6	249.0	0.94	211.7	0.80	230.5	0.87
UH10NN	573.0	518.9	0.91	541.5	0.95	529.5	0.92
UH10F1	245.0	259.9	1.06	206.8	0.84	243.9	1.00
UH10F2	198.5	227.3	1.15	164.9	0.83	218.4	1.10
UH10F3	155.0	194.7	1.26	122.9	0.79	192.4	1.24
UH10T3	185.0	221.5	1.20	168.4	0.91	210.0	1.14
UH10S3	140.0	181.8	1.30	98.8	0.71	184.4	1.32
UH15NN	418.0	420.3	1.01	384.8	0.92	411.6	0.98
UH15F3	94.8	145.1	1.53	15.9	0.17	161.0	1.70
L5NN	500.0	478.2	0.96	528.6	1.06	402.4	0.80
LFF3C	233.2	232.2	1.00	224.4	0.96	151.8	0.65
L10NN	375.0	373.5	1.00	387.6	1.03	282.4	0.75
L10F3C	117.1	129.4	1.11	90.6	0.77	87.4	0.75
Average			1.00		0.84		0.93
Standard Deviation			0.18		0.15		0.21